Transient-State Kinetic Analysis of *Synechococcus* Glutamate 1-Semialdehyde Aminotransferase†

Marvin A. Smith,* Peter J. King,‡ and Bernhard Grimm§

Department of Chemistry and Biochemistry, Brigham Young University, Provo, Utah 84602, Applied Photophysics Ltd., Leatherhead KT22 7PB, U.K. and Institut für Pflanzengenetik and Kulturpflanzenforschung, Corrensstrasse 3, D-06466 Gatersleben, Germany

Received July 18, 1997; Revised Manuscript Received October 20, 1997⊗

ABSTRACT: We report a transient-state kinetic analysis relating to the mechanism of glutamate 1-semialdehyde aminotransferase (GSAT). Multiple-wavelength spectral kinetic data were collected by microstopped-flow spectrophotometry. Time resolved spectral sketches resulting from reactions with glutamate 1-semialdehyde (GSA), 4,5-diaminovalerate (DAVA), and 5-aminolevulinate (ALA) indicated various transient chromophoric intermediates. On the basis of the generally accepted mechanism of other aminotransferases and absorbance characteristics of associated intermediates, these transient chromophores are likely associated with Schiff base formation, ketimine/aldimine tautomerization, and transimidation etc. Spectral kinetic changes associated with these putative intermediates were, in general, concentration dependent. Various experimental evidence, including reactions with the GSAT lys272ile mutant, suggested rapid equilibrium of isomeric aldimines and geminal diamines. With this and related simplifying assumptions, a minimal mechanism was derived which provided a means for transient-state spectral kinetic analysis of reactions with GSA, DAVA, and ALA, all of which lead to the formation of the same putative central enzyme complex. Resulting kinetic constants were internally consistent, in general agreement with steady-state and equilibrium data (K_M, k_{cat}, and K_{eq}), and provided the basis for a reasonable computer simulation of the original data set (variance $\approx 4 \times 10^{-5}$). Reequilibration of enzyme intermediates following an apparent pseudoequilibrium indicated thermodynamically driven dissociation of the central aldiminic enzyme complex. This is consistent with previous observations and the minimal mechanism used in this kinetic analysis and suggests a plausible regulatory mechanism of GSAT.

GSAT [(*S*)-4-amino-5-oxopentanoate 4,5 aminotransferase, EC 5.4.3.8] is the last of three enyzmes involved in the metabolic conversion of glutamate to 5-aminolevulinate (ALA)[1] (*1*, *2*). This metabolic sequence is of particular interest because of its role in light regulation of tetrapyrrole biosynthesis in photosynthetic organisms (*3*). GSAT is related to other aminotransferases (*4*−*7*). It has an absorption spectrum typical of vitamin B_6-containing enzymes and can be interconverted between its aminic (pyridoxamine-5′-phosphate, ∼338 nm) and aldiminic (pyridoxaldimine-5′-phosphate, ∼418 nm) forms by various amino and oxo acids. However, GSAT is unique in that no other amino or oxo acid is required in the conversion of its natural substrate glutamate 1-semialdehyde (GSA) to ALA. GSAT is thus a mutase which catalyzes the net intramolecular transfer of amino and carbonyl functions of GSA via its pyridoxamine-5′-phosphate cofactor. Ketimine-aldimine tautomerization (*8*) is mediated by acid/base interconversion of Lys272 (*9*). The enzymic mechanism purportedly consists of two half-reactions in which 4,5-diaminovalerate (DAVA) or its geminal diamine is a likely intermediate. Supporting evidence is based on typical ping-pong bi-bi kinetics with DAVA as the second substrate (*7*). Kinetic experiments with GSAT are complicated by substrate instability, and the reactivity of both aminic and aldiminic enzyme forms with both enantiomers of GSA and with ALA (*6*, *7*). (*R*)GSA, (*R*,*S*)DAVA, and ALA appear to induce only single turnover half-reactions. Approximately half of racemic GSA is quantitatively converted to ALA (*6*), probably the *S* enantiomer. Although tautomeric interconversions (ketimine/aldimine) have been observed with this enantiomer, spectrophotometric reactions are rapid and mixtures of transient intermediates too complex for kinetic analysis by conventional spectrophotometry (*6*). Further mechanistic characterization has also been hampered by the lack of tertiary structural data and unavailability of analogues and radioactive substrates. In the present communication, we have used stopped-flow spectrophotometry and transient-state kinetic theory for kinetic analysis of mechanistic reactions of GSAT.

† Supported in part by Brigham Young University, and a grant from the EC Human Capital and Mobility Programme 1991−94 (CHRX-CT93-0179) given to B.G.

* Author to whom correspondence should be addressed.

‡ Applied Photophysics Ltd.

§ Institut für Pflanzengenetik and Kulturpflanzenforschung.

⊗ Abstract published in *Advance ACS Abstracts,* December 1, 1997.

[1] Abbreviations: GSAT, glutamate 1-semialdehyde aminotransferase; E_L and E_M are the aldiminic or pyridoxaldimine-5′-phosphate and aminic or pyridoxamine forms of GSAT; GSA, glutamate 1-semialdehyde; ALA, 5-aminolevulinate; DAVA, 4,5-diaminovalerate; DOVA, 4,5-dioxovalerate.

S0006-2960(97)01758-3 CCC: $15.00
Published on Web 01/06/1998

Scheme 1

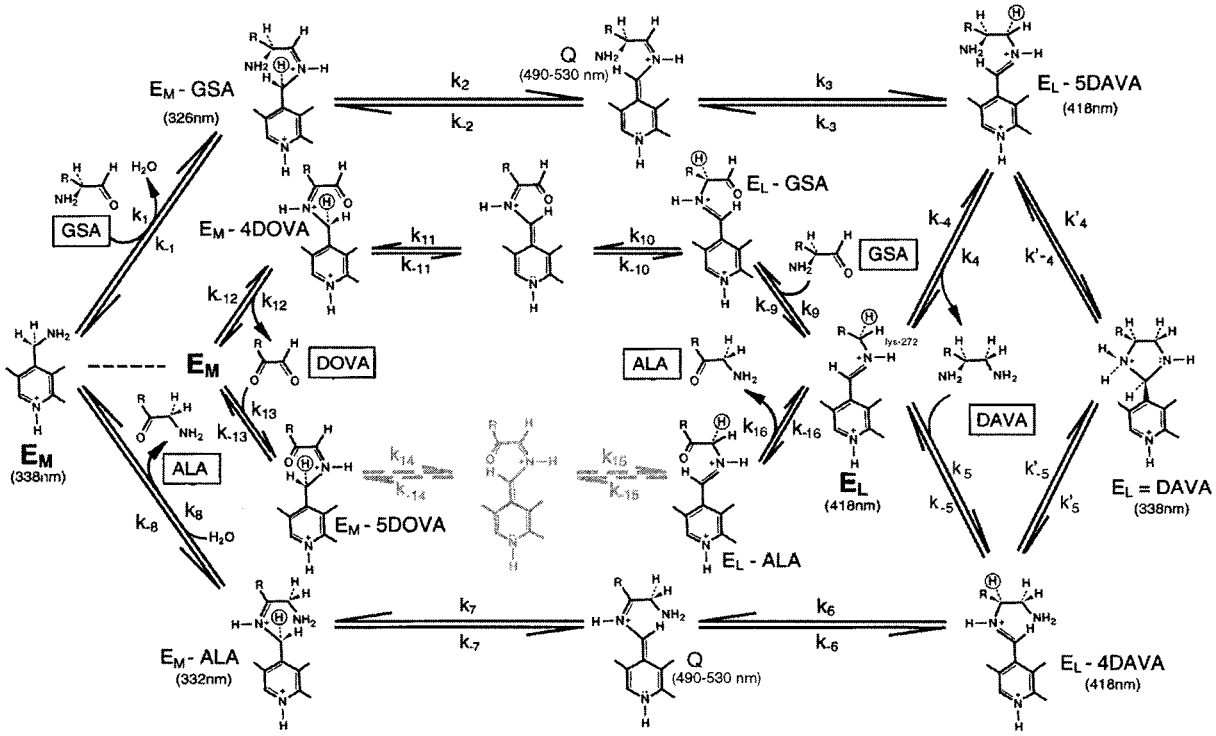

EXPERIMENTAL PROCEDURES

Chemicals. (*S*)GSA was synthesized and purified as previously described (*10*). 4-Aminohex-5-enoate used in this preparation was generously provided by Marrion Merrell-Dow, Strasbourg, France; ALA, DAVA (γ-ornithine) and succinate semialdehyde were obtained from Sigma.

GSA-Aminotransferase. Synechococcus GSAT was purified to near homogeneity from lysates of transformed *Escherichia coli* (*11*). The enzyme was converted to aminic and aldiminic enzyme with DAVA and succinate semialdehyde, respectively (*7*, *12*).

Spectrophotometric Analyses. Spectrophotometric analyses were typically carried out between 20 and 25 °C, in Tricine, 100 mM, pH 7.9. Active enzyme concentrations (6.7−50 μM) were determined from coenzyme molar extinction coefficients of purified protein at 338 or 418 nm (*7*). In general, the concentration dependance of apparent rate constants was determined under conditions of pseudo-first-order kinetics, where substrate to enzyme concentration ratios were more than an order of magnitude. At lower substrate concentrations, these criteria were difficult to maintain. Nevertheless, a reasonably consistent fit to appropriate rate equations was obtained using experimental substrate concentrations decreased by an amount equal to that of GSAT.

Multiple-wavelength kinetic data were collected with an SX17MV stopped-flow system (Applied Photophysics Ltd., Leatherhead, U.K.) at 5−10 nm intervals. Rate constants were determined by simultaneous multiple exponential fitting of single wavelength transient data sets, and evaluated by the magnitude of the standard error and randomness of time-dependent residuals. Reaction modeling and global analysis were performed using Pro-Kineticist software. This was used both to simulate artificial data sets for comparison with experimental measurements and, where feasible, to fit and refine rates and absorption spectra globally. Introduction of known spectra and fixed rates provided sufficient constraints to allow successful fitting to a minimal mechanism.

Reactions of GSAT. On the basis of the generally accepted mechanism of transamination (*13*, *14*), one might expect GSAT to catalyze the following reactions with its natural substrate GSA, Scheme 1. This scheme is consistent with numerous experimental observations, primarily with GSAT (*6*, *7*, *9*, *12*, *15*). Reactions 1−8 (identified by rate constants, k_n, having subscripts with the same numerical designation) are shown in the outer perimeter. They represent reactions of (*S*)GSA with the pyridoxamine-5′-phosphate form of the enzyme (aminic or E_M) leading to the formation of the product ALA, as previously described (*16*). Clockwise, they include (1) Schiff base (E_M-GSA) formation; (2 and 3) tautomerization through quinonoid related resonance-stabilized intermediates (Q) leading to formation of the C-5 external aldimine of DAVA (E_L-5DAVA); (4 and 5) transimidation resulting in the isomerization of C-5 and C-4 external aldimines of DAVA, via either the internal aldimine of GSAT (E_L) or (4′ and 5′) the cyclic imidazolidine of DAVA (E_L═DAVA); (6 and 7) a second tautomerization; and (8) ketimine (E_M-ALA) hydrolysis.

Reactions 9−16 shown counterclockwise in the inner circle of the scheme represent an analogous set of reactions of GSA but with the pyridoxaldimine-5′-phosphate form of GSAT (aldiminic or E_L). Diaminovalerate (DAVA) and dioxovalerate (DOVA), the expected intermediates according to this scheme, are obtained by transimidization and hydrolysis (reactions 4 and 12, respectively). In general, the aminic and aldiminic enzyme forms of GSAT are represented by E_M and E_L, respectively. Enzyme intermediates of the type E_M−X or E_L−X are condensation products, i.e., ketimines or aldimines. Q represents resonance-stabilized quinonoid related intermediates, and E_L═DAVA the cyclic imidazolidine (geminal diamine) of DAVA with E_L (*16*). R = $-CH_2$-

Scheme 2

$$
\begin{array}{l}
E_M + GSA \\
\quad (1)\ \uparrow\downarrow \\
E_M\text{-}GSA \\
(2\&3)\uparrow\downarrow \qquad (4 \text{ or } 5) \\
(\mathbf{E_L\text{-}X}) \rightleftarrows E_L + DAVA \\
(6\&7)\uparrow\downarrow \\
E_M\text{-}ALA \\
\quad (8)\ \uparrow\downarrow \\
E_M + ALA
\end{array}
$$

CH_2COO^-. No direct evidence has been obtained for reactions 14 and 15, represented by dashed arrows, except in the presence of added nitrogenous base. Suggested approximate absorption maxima (λ_{max}) are as indicated.

Establishing a Minimal Kinetic Scheme. Most of the reactions in Scheme 1 can be expected with (*S*)GSA as the only substrate. The sheer number of these reactions and the expected spectral similarity of various enzyme intermediates would seem to preclude a reasonable kinetic analysis. However, based on various experimental observations and under appropriate conditions, the following simplifying assumptions can be justified. First, secondary reactions of GSA and ALA with aldiminic GSAT (E_L) (Scheme 1, beginning with reactions 9 or 16) are probably insignificant in transient- and pre-steady-state experiments where initial concentrations of this enzyme form and GSA or ALA are negligible. Second, we have assumed that external aldimines of DAVA, and enzyme intermediates involved in their interconversion (reactions 4′ and 5′), are in rapid equilibrium (see later in Results). On the basis of this assumption, these intermediates can be combined as a single heterologous enzyme complex (E_L-X) with characteristics defined by equilibrium concentrations of constituent enzyme forms. This leads directly to the last (third) important simplifying assumption that spectrophotometric changes observed in the enzymic conversion of GSA to ALA are primarily a consequence of transient binary enzyme intermediates, such as those represented by reactions 1−8 in the outer perimeter of Scheme 1. Taken together, these assumptions form the basis of the following minimal reaction mechanism (Scheme 2).

Reaction numbers and symbols correspond with those of Scheme 1. Quinonoid related intermediates apparently do not accumulate (*6*), and therefore, steps involving their formation have been combined for simplification (reactions 2 and 3 and 6 and 7). In addition, all covalent binary external aldimine and geminal diamine enzyme intermediates have been combined in a single complex represented by (E_L-X).

Calculation of Kinetic Constants. Our general approach has been to study the concentration dependence of reactions leading to the formation of the putative central enzyme complex (E_L-X) beginning with (a) the reactant GSA, (b) the product ALA, or (c) the intermediate DAVA, Scheme 2. Pre-steady-state spectral changes associated with the enzymatic reaction of GSA are best fit to a triple exponential. Because the apparent rate constant of the fast phase of this reaction increases linearly without signs of saturation (Figure 3A) there is little information to define the binding of GSA in the initial collision complex. On the basis of the minimal mechanism, we have assumed a simple two-step reversible sequence leading to the formation of E_L-X and fit the fast

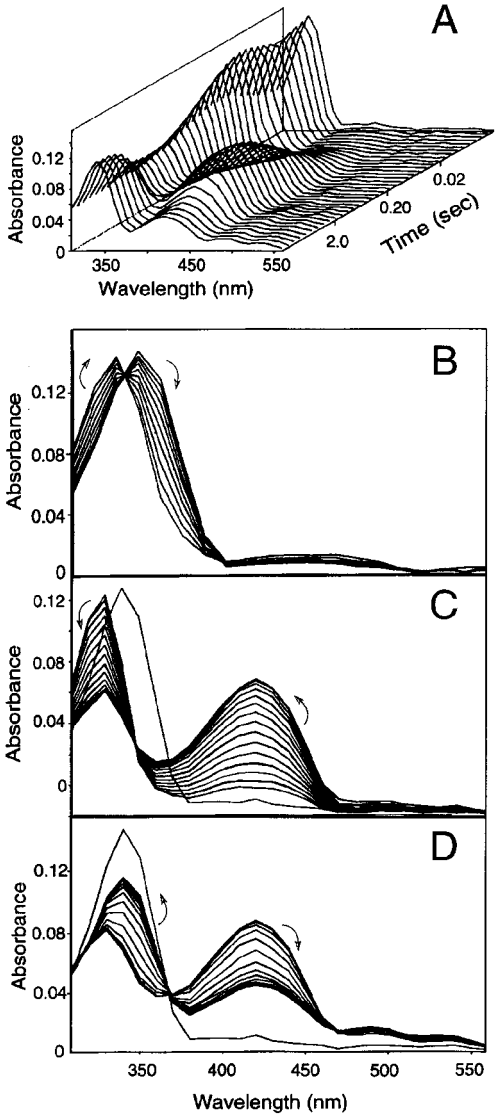

FIGURE 1: Spectral kinetic analysis of the reaction of GSA aminotransferase with GSA. Multiwavelength kinetic data were collected at various fixed wavelengths (10 nm intervals from 310−560 nm) upon rapid mixing of equal volumes of (*S*)GSA and the aminic form (E_M) of GSA aminotransferase, at 20 °C, using a 4 decade log time base ranging from 0 to 20 s (final concentrations were 500 and 25 μM, respectively). Data sets were collected and analyzed by microvolume stopped-flow spectrophotometry and associated software (SX.17MV, Pro-Kineticist, Applied Photophysics, Ltd.) (A) 27 of 900 three dimensional time-resolved spectral sketches, transformed from original multiple wavelength kinetic data sets. (B) Overlays of spectral sketches generated during the first apparent spectral change (3−50 ms). λ_{max} of the initial aminic enzyme shifted to shorter wavelengths (∼338 → 326 nm) at an apparent exponential rate ($k_{app} \approx 50\ s^{-1}$) with an isosbestic point at ∼334 nm. (C) Overlays of spectral sketches generated during the second apparent spectral change (60−1500 ms). The 326 nm enzyme form was converted to aldimine-like intermediate(s) (418 nm) ($k_{app} \approx 4\ s^{-1}$) having an isosbestic point at 348 nm. The 3 ms spectrum is shown for comparison. This spectral shift is actually best-fit to a double exponential (Figure 2A). (D) Overlays of spectral sketches generated during the third apparent spectral change (2−20 s). Aldimine-like intermediates (418 nm) were converted back to aminic-like GSAT (338 nm) at an apparent exponential rate ($k_{app} \approx 0.5\ s^{-1}$) with an isosbestic point at ∼369 nm. A second isosbestic point at 468 nm implicates quinonoid-related intermediates (∼490−530 nm) in this conversion, i.e., aldimine → quinonoid → ketimine. Although such intermediates are considered integral to the reaction mechanism, they do not accumulate significantly in the enzymic conversion of GSA to ALA. The 3 ms spectrum is shown for comparison.

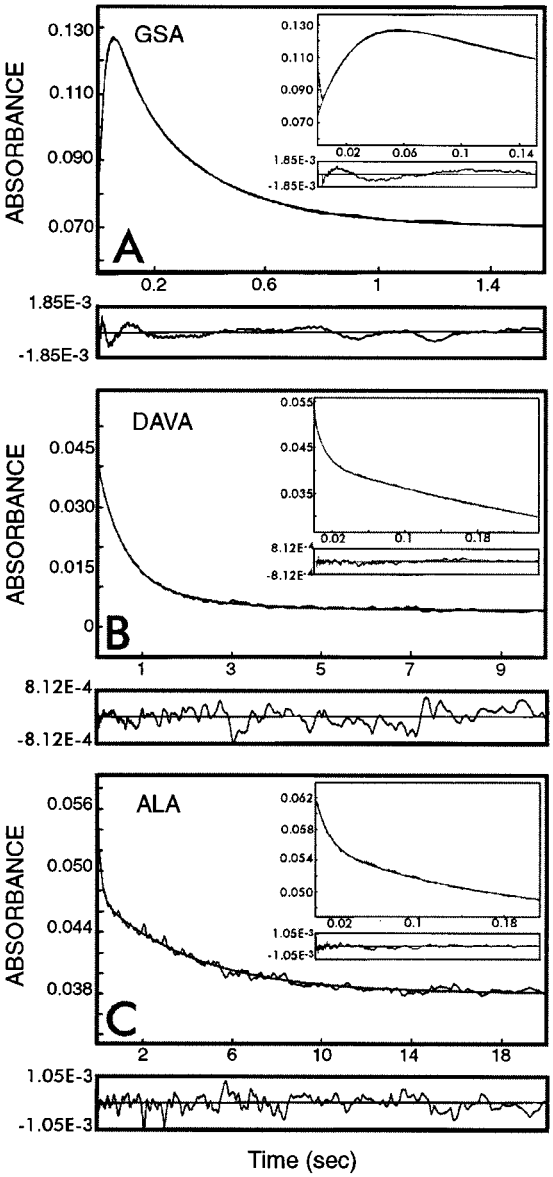

FIGURE 2: Time-dependent absorbance of GSAT upon rapid mixing with GSA, DAVA, or ALA. Rates were fitted to a triple exponential. Resulting residuals for each reaction are as shown. (Insets) Zoom of early reaction stages. (A) Pre-steady-state spectral changes of aminic GSAT at 320 nm upon rapid mixing with (*S*)GSA (apparent rate constants = 32, 17, 3 s^{-1}). Conditions were essentially as described in Figure 1. (B) Spectral changes of aldiminic GSAT at 420 nm upon rapid mixing with (*R*,*S*)DAVA (apparent rate constants = 80, 2, 0.6 s^{-1}). Final concentrations of (*S*)DAVA and GSAT were 125 and 10.2 μM, respectively. (C) Spectral changes of aminic GSAT at 350 nm upon rapid mixing with ALA (apparent rate constants = 81, 7, 0.2 s^{-1}). Final concentrations of ALA and GSAT were 9600 and 6.7 μM, respectively.

and the intermediate apparent rate constants (k_{1obs}, k_{2obs}, respectively) to the following equations (*17*).

$$k_{1obs} \approx k_{+1}[S] + k_{-1} + k_{+2} + k_{-2} \quad (1)$$

$$k_{2obs} \approx \frac{k_{+1}[S](k_{-2} + k_{+2}) + k_{-1}k_{-2}}{k_{+1}[S] + k_{-1} + k_{+2} + k_{-2}} \quad (2)$$

The substrate concentration dependence of k_{1obs} was fit to a straight line, while that of the intermediate apparent rate constant (k_{2obs}) approximated a rectangular hyperbola, with

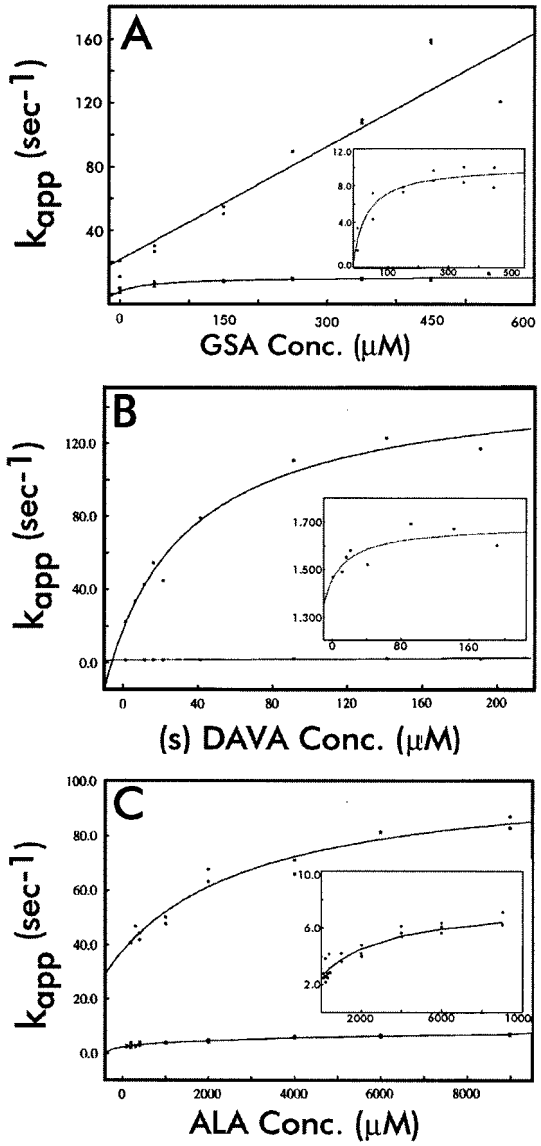

FIGURE 3: Concentration dependence of apparent rate constants for reactions with GSA, DAVA, and ALA. Conditions were essentially as described in Figure 2. Rate constants were calculated at various fixed concentrations by averaging data sets at indicated wavelengths and fitting to either a straight line or a rectangular hyperbola, as described in Experimental Procedures. (Insets) Zoom of smaller apparent rate constants (k_{2obs}). (A) Reactions of GSA with aminic GSAT at 340 and 345 nm. (B) Reactions of DAVA with aldiminic GSAT at 420 nm. (C) Reactions of ALA with aminic GSAT at 330, 350, and 420 nm.

the apparent dissociation constant ($K_{d,app}$) defined by the following equation.

$$K_{d,app} \approx k_{-1}k_{-2}/k_{+1}(k_{+2} + k_{-2}) = K_d\, k_{-2}/(k_{+2} + k_{-2}) \quad (3)$$

k_{3obs} showed no consistent pattern of concentration dependence.

Reactions of DAVA and ALA were similar except saturation of the fast phase suggested initial formation of a collision complex followed by two first-order transitions (Figure 3, panels B and C). Thus, a simple three-step reversible scheme was used in which formation of collision complex was assumed to be in rapid equilibrium. Apparent rate constants (k_{1obs} and k_{2obs}) were fit to the following relationships (*18, 19*).

$$k_{1obs} \approx \frac{K_0[S]k_{+1}}{(K_0[S]+1)} + k_{-1} + k_{+2} + k_{-1} \quad (4)$$

$$k_{2obs} \approx \frac{\dfrac{K_0[S]k_{+1}(k_{+2}+k_{-2})}{(K_0[S]+1)} + k_{-1}k_{-2}}{\dfrac{K_0[S]k_{+1}}{(K_0[S]+1)} + k_{-1} + k_{+2} + k_{-2}} \quad (5)$$

Fitting k_{2obs} to a rectangular hyperbola leads to an expression for the equilibrium constant (K_0) of putative collision complexes.

$$K_0 \approx k_{-1}k_{-2}/K_{d,app}k_{+1}(k_{+2}+k_{-2}) \quad (6)$$

Complete solution of k_{1obs} and k_{2obs} for GSA, DAVA, and ALA, using limiting values at both extremes of concentration scales (Figure 3), provided a means for obtaining slopes, limiting-slopes, k_{obs}-intercepts, and k_{obs}-maxima, from which numerical values for each of the rate and equilibrium constants were directly calculated.

Spectrophotometric changes observed upon rapid mixing of GSAT with each of these substrates are attributable to alterations in specific conjugated bonding patterns with the coenzyme. Therefore, characteristic vitamin B_6-associated spectral kinetic changes are sensitive reporters of transient intermediates integral to the overall enzyme mechanism.

RESULTS

The reaction mechanism of glutamate 1-semialdehyde aminotransferase (GSAT) has been investigated using microstopped-flow spectrophotometry. Transient-state kinetic theory provided the basis for calculating parameters which define the kinetic characteristics of intermediates observed during the reaction. These parameters were subsequently applied to the minimal mechanism (Scheme 2) defined largely by the generally accepted mechanism of other aminotransferases (*13*, *14*), singular value decomposition factor analysis, and the spectral characteristics of expected enzyme intermediates. The kinetic analysis begins at the ends of the pathway [with the individual reactions of (*S*)-GSA, ALA, or (*R*,*S*)DAVA] and works toward the putative central enzyme complex (E_L-X).

Spectral Kinetic Sketches of the Reaction of GSA-Aminotransferase. Multiple-wavelength kinetic data (collected at 5−10 nm intervals from 310−560 nm) were obtained upon rapid mixing of each substrate with *Synechococcal* GSAT using a 4 decade log time base.

For example, spectral changes which occur upon equilibration of the natural substrate (*S*)GSA (0.50 mM, ∼8 × K_M) with the enzyme are illustrated in Figure 1. In part A, multiple-wavelength time-dependent absorptivities were transformed to time-resolved spectral sketches. In this equilibration, which leads to the near quantitative conversion of GSA to the product ALA, three major spectral shifts are apparent. The first two precede steady state, while the third represents its collapse and approaching equilibrium. Each of these three apparent changes has been isolated in time and displayed as spectral overlays.

Spectral changes observed during the first ∼50 ms with (*S*)GSA are illustrated in Figure 1B. The λ_{max} of native aminic GSAT (338 nm) shifted to a shorter wavelength (326 nm) at an exponential rate ($k_{app} \approx 50\ s^{-1}$) with an isosbestic point at ∼334 nm. A second major spectral change was observed between ∼60 and 1500 ms (Figure 1C). It is characterized by the subsequent shift of λ_{max} (326 nm) to a longer wavelength (418 nm). Although not immediately apparent, this reaction is best fit to a double exponential, as will be explained later. The major component ($k_{app} \approx 4.0\ s^{-1}$) has an isosbestic point at ∼348 nm. The 3 ms spectrum from Figure 1B, which is indistinguishable from that of the initial aminic enzyme (λ_{max} = 338 nm), is shown for comparison. In a third spectral change, which is unique to reactions with GSA, λ_{max} of the aldimine-like intermediate-(s) (∼418 nm) was shifted back to the wavelength of the original aminic enzyme (∼338 nm). This exponential reaction occurs between ∼2 and 20 s ($k_{app} \approx 0.52\ s^{-1}$) with an isosbestic point at ∼369 nm (Figure 1D). The spectrum of the initial aminic enzyme is again shown for comparison (3 ms spectrum). Apparent rate constants described above could be obtained from spectral changes observed at any of several characteristic wavelengths, i.e., for GSA at 310, 320, 330, and 360 nm, etc.

These results are consistent with rate-limiting proton extraction (*20*), in which case the first spectral change is likely associated with accumulation of condensation products (Schiff base), and the second with accumulation of the central aldimine-like enzyme complex (E_L-X) and perhaps transient equilibration with aldiminic enzyme E_L and DAVA (Scheme 2, side reaction). Accordingly, the final spectral change is associated with collapse of steady state and return of GSAT to the aminic E_M form.

Similar spectral changes were also observed upon rapid mixing of ALA and (*R*,*S*)DAVA with aminic and aldiminic GSAT, respectively. The general characteristics of these reactions reflected those described above for GSA, with the notable distinction that no steady-state turnover and collapse was observed, i.e., only two major spectral changes were apparent, presumably Schiff base formation and ketimine/aldimine tautomerization (described later, Figure 4A). This was anticipated in the case of DAVA because no amino-accepting substrate was present. However, in the reverse reaction, with the product ALA, equilibration appeared to be associated with accumulation of aldimine-like enzyme intermediates. Spectrophotometric differences in reactions of GSA and ALA, and the relatively high concentration of ALA required (∼20× higher), are a direct reflection of thermodynamic differences between the two half reactions, i.e., GSA ⇌ DAVA and DAVA ⇌ ALA. They confirm that the overall reaction greatly favors ALA synthesis (*7*).

Single-Wavelength Kinetic Analyses of Reactions with GSA, DAVA, and ALA. In general reactions of each of these substrates with aminic (E_M) or aldiminic (E_L), GSAT (pre-steady-state in the case of GSA) were best-fit to triple exponentials, suggesting at least four spectrally distinct enzyme forms. The pre-steady-state portion of the reaction with GSA was monitored at several different wavelengths with similar results. At 320 nm, the formation and demise of the first apparent enzyme intermediate is observed, Figure 2A. The absorbance rapidly increased and then gradually decreased. The inset shows the initial ∼140 ms of reaction. Residuals are those obtained upon fitting to a triple exponential (normal variance = 2.53×10^{-7}). Nonrandom

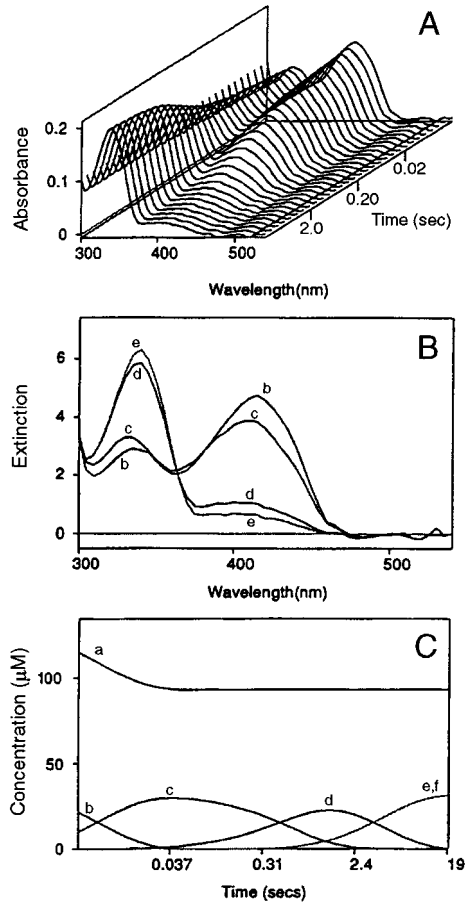

FIGURE 4: Spectral kinetic analysis of the reaction of GSA aminotransferase with DAVA. (A) Multiwavelength kinetic data collected at various fixed wavelengths (5 nm intervals from 310−560 nm) upon rapid mixing of equal volumes of (*R*,*S*)DAVA (250 μM) and the aldiminic form (E_L) of GSAT (64 μM) at 20 °C, using a 4 decade log time base. Data sets were collected and analyzed as described in Figure 1. Decay at 420 nm was best fit to a triple exponential ($k_{app} \approx 83$, 1.8, and 0.6 s^{-1}, respectively). Therefore, data sets in panel A were fit to the following minimal mechanism: a + b $\rightleftarrows$ c $\rightleftarrows$ d $\rightleftarrows$ e + f (variance = 1.6×10^{-7}). Substrate a and product f were assumed colorless. Introduction of approximate rates for each reversible step of the reaction provided sufficient constraint to allow successful reaction modeling. (B) Artificial calculated spectra of curves b−e resulting from above global analysis. (C) Time-dependent concentration profiles of each enzyme intermediate represented in panel B.

variations during initial stages of the reaction are likely mixing artifacts.

The reaction of DAVA with GSAT was similarly monitored at several different wavelengths. Decay of the initial aldiminic-like enzyme (E_L at 420 nm) was likewise best-fit to a triple exponential, Figure 2B. Amplification of early stages of the reaction (inset) and corresponding residuals are also shown (normal variance of 2.90×10^{-8}).

The reverse reaction with ALA and aminic enzyme (E_M) is shown at 350 nm, Figure 2C, along with residuals to a triple exponential fit (normal variance = 4.94×10^{-8}).

Concentration Dependence of Apparent Rate Constants in Reactions with GSA, DAVA, and ALA. Transient-state kinetic theory relies on information derived from the concentration dependence of observed rate constants. The smallest of the three observed rate constants (k_{3obs}), derived by simultaneous multiple fitting to triple exponentials as described above, did not indicate a consistent concentration dependence in the ranges tested. In contrast, the larger constants (k_{1obs} and k_{2obs}) were concentration dependent. The largest observed rate constant (k_{1obs}) for GSA increased linearly with a slope of 0.236 s^{-1} μM^{-1} and an intercept of 21.5 s^{-1}, Figure 3A. All other concentration-dependent rates approached maximum values with increasing substrate concentrations. These were fit to a rectangular hyperbola (Figure 3), which provided the basis for calculating intrinsic rate constants as described in Experimental Procedures. Resulting k_{1obs} minima (*y*-intercepts) and maxima for DAVA and ALA (Figure 3, panels B and C) were 18 and 153 s^{-1}, and 38 and 102 s^{-1}, respectively. Calculated k_{2obs} intercepts and maxima for GSA, DAVA, and ALA, were 1.49 and 10.1, 1.46 and 1.69, and 2.52 and 7.98 s^{-1}, respectively.

Rapid Equilibrium between Aldimines and Geminal Diamines of GSAT. Attempts to derive a minimal mechanism by simulating the enzymic isomerization of GSA (Scheme 1) proved to be very complex. However, the reaction initiated with DAVA and aldiminic GSAT (E_L) (Figure 4A) resembles half-reactions obtained with other aminotransferases. Spectrophotometric changes observed in this reaction with DAVA were simulated (Pro-Kineticist) using a simple, linear, three-step, reversible mechanism (a + b $\rightleftharpoons$ c $\rightleftharpoons$ d $\rightleftharpoons$ e + f) (variance = 1.6×10^{-7}). Resulting artificial calculated spectra and associated time-dependent concentration changes are shown, Figure 4, panels B and C. Nearly identical results were obtained in simulating the reaction of ALA with aminic GSAT (E_M), except characteristic spectra were observed in the reverse time sequence (data not shown). Substrate and product are represented by a and f and were assumed to be colorless, while various enzyme forms are represented by b−e. Calculated spectra of curves b and e are indistinguishable from and assumed to represent E_L and E_M, respectively, although collision complexes with DAVA and ALA or related conformers have not been eliminated. The intermediate d is likely the ketimine of ALA (compare with Figure 1B). This being the case, we are left with the complex c (dubbed E_L−X) with maxima at ~332 and 415 nm. In reactions with ALA, absorptivities at these maxima are nearly equal (data not shown), while in the case of DAVA, relative absorption at 415 nm is somewhat larger.

Time-dependent concentration decreases (Figure 4C) show near quantitative combination of a (DAVA) and b (GSAT) with concomitant increases in a mixture of absorbing species c (~40 ms), which are subsequently converted to d (~1 s) and then e + f (~20 s).

A mixture of coenzyme absorbing species with maxima similar to those described above (spectrum c) were previously obtained in spectral kinetic reactions of enzyme free pyridoxal-5′-phosphate with ethylene diamine. These intermediates were identified as the corresponding pyridoxaldimine in rapid equilibrium with its cyclic geminal diamine (*15*). Accordingly, the transient appearance of c during initial stages of the reaction with DAVA and its calculated spectrum suggested a heterologous enzyme intermediate, perhaps related to the external aldimine of DAVA. This possibility prompted equilibrium titration and kinetic experiments with enzyme-free pyridoxal-5′-phosphate (PLP) and DAVA. Spectra similar to those of E_L−X and the bimodal intermediates of ethylenediamine were again observed (data not shown), suggesting rapid equilibrium between related intermediates, such as external aldimines (~418 nm) and cyclic

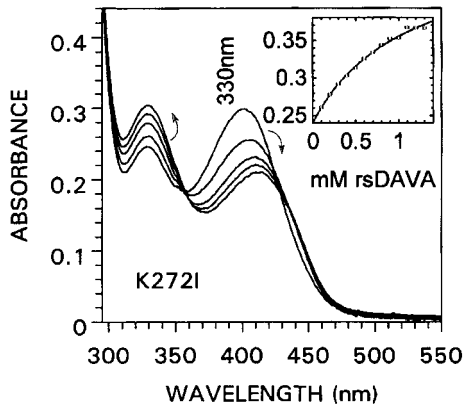

FIGURE 5: Equilibrium-titration of the Lys272Ile GSAT mutant with DAVA. A 1.0 mL buffered solution (0.1 M Tricine, 1 mM $MgCl_2$, 1mM DTT, pH 7.9) of the pyridoxal form of mutant GSAT (56 μM) (Grimm et al., 1992) was titrated at room temperature with 1 μL additions of 100 mM (*R*,*S*)DAVA. Spectra were recorded (Beckman Diode Array, 7400) after addition of DAVA upon attainment of spectral equilibrium. Absorbance decreases at ~390 nm (pyridoxal form of mutant GSAT) occur with simultaneous increases at ~330 (putative cyclic diamine) and 415 nm (aldiminic GSAT) with isosbestic points at ~360 and 445 nm. (Inset) DAVA concentration dependent changes at 330 nm.

geminal diamines (~338 nm) as initially shown by Tobias and Kallen (*15*).

The most convincing evidence that this putative heterologous complex (E_L-X) is directly involved in GSAT catalyzed reactions was obtained with the Lys272Ile mutant. This site-directed mutant is catalytically inactive because Lys-272 is essential for internal aldimine formation and tautomeric 1,3-prototropic rearrangements. Nevertheless, external aldimines (~418 nm) are obtained in reactions with GSA and ALA, each of which contains only a single amino group (*9*). In equilibrium titration reactions with DAVA, which has both a C-4 and a C-5 amino group, two absorbance maxima are obtained, Figure 5. The absorbance maximum of the pyridoxal enzyme form (~390 nm) decreased and shifted to longer wavelengths (~415 nm, aldimine) with concomitant increases at ~330 nm (putative cyclic geminal diamine) and isosbestic points at ~360 and 445 nm. The concentration dependence of this reaction was fit to a model for a single binding site (Figure 5, inset) giving a K_d of ~1 mM. On the basis of these experimental results, we conclude that the E_L-X complex likely represents the external aldimine and cyclic geminal diamine of DAVA in rapid equilibrium and that this imidazolidine is directly involved in the enzymic conversion of GSA to ALA, as previously suggested (*7*,*16*). This is entirely consistent with Tobias and Kallen (*15*), who conclude that the pathway for intramolecular transimidation via a geminal diamine is extremely rapid and may not require catalysis except perhaps for entropic contributions.

Calculation of Rate and Association Constants for Mechanistic Reactions of GSA. On the basis of the above experiments and extensive observations with GSAT and other amino transferases (*14*), it is not unreasonable to assume that the 338 → 418 nm spectral shift observed by stopped-flow spectrophotometry (Figure 1C) is associated with acid/base catalyzed tautomeric rearrangement. Similar spectral changes are observed with GSAT upon coenzyme replacement (pyridoxamine-5′-phosphate replacement with pyridoxal-5′-phosphate results in the change of λ_{max} from ~338 to 418 nm, data not shown). Single turnover half-reactions with unrelated substrates such as succinate semialdehyde and DOVA are also consistent with this assumption (data not shown).

Scheme 3

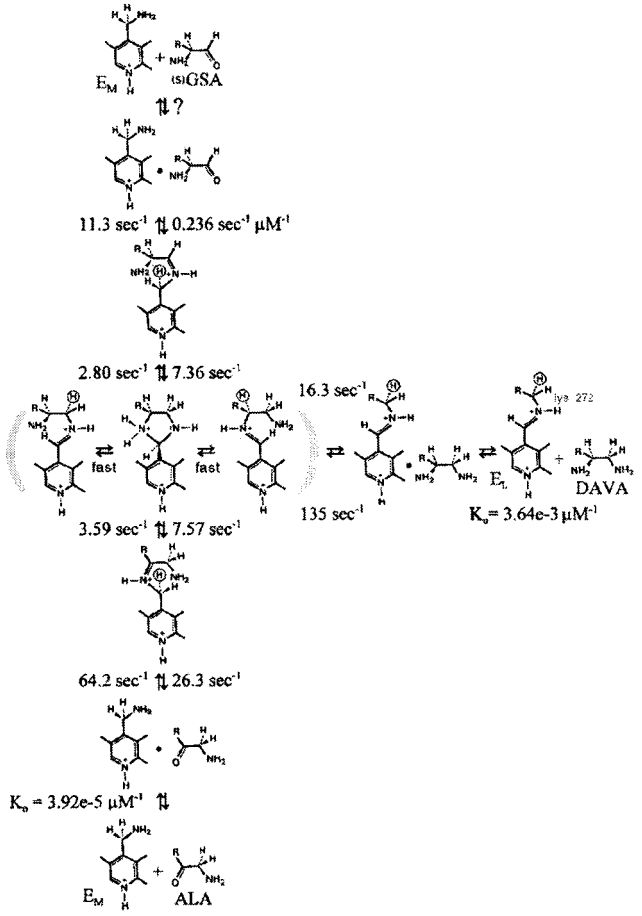

It is tempting therefore to associate the characteristic spectral change which immediately precedes such tautomeric rearrangements (e.g., Figure 1B) with formation of condensation products such as aldimines or ketimines. Furthermore, hyperbolic increases of apparent rate constants (k_{1obs}) in the case of DAVA and ALA (Figure 3, panels B and C, respectively) could logically be associated with collision complex formation, although associated hydration/dehydration reactions and conformational changes, etc., have certainly not been eliminated.

Accordingly, rate and association constants calculated from concentration-dependent data (Figure 3) using transient-state kinetic theory (Experimental Procedures, eqs 1−6) were directly substituted into a minimal reaction mechanism, as shown in Scheme 3. Symbols are as previously explained (Scheme 1), with the exception that E_M·GSA or E_M·ALA and E_L·DAVA represent collision complexes with aminic and aldiminic enzyme forms, respectively.

Computer Simulation of the Minimal Reaction Mechanism of GSAT. The validity of this minimal mechanism and associated constants was evaluated in part by computer simulation using the following simple branched mechanism: a + b ⇌ c ⇌ d ⇌ g ⇌ b + h and d ⇌ e + f (compare with Schemes 2 and 3) (Pro-Kineticist, Applied Photophysics Ltd). Introduction of fixed rates and a minimal number of

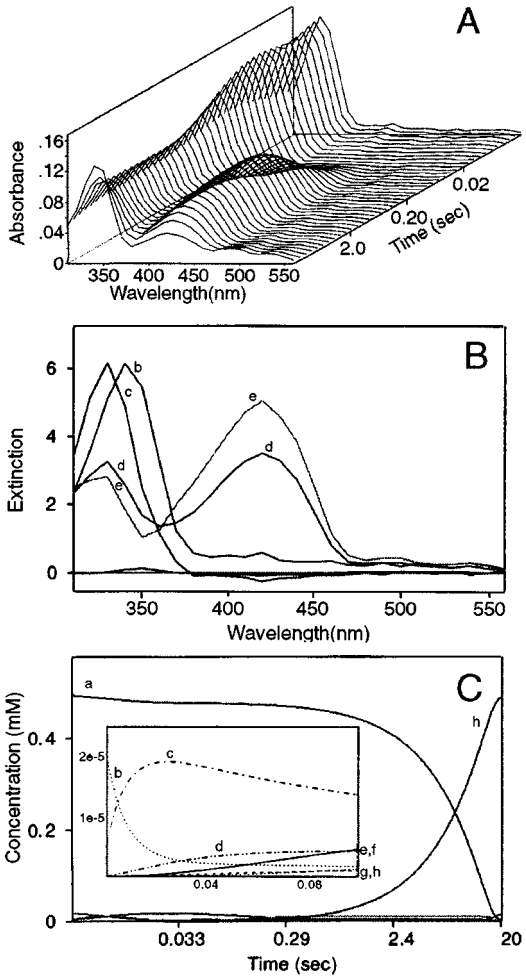

FIGURE 6: Simulation of the reaction of GSA aminotransferase with GSA. (A) Time-dependent spectral changes observed during the enzymic conversion of GSA to ALA (Figure 1A) were simulated (Pro-Kineticist Applied Photophysics, Ltd.) using the minimal mechanism and associated constants derived from transient-state kinetic theory (Scheme 3) (variance = 4.16×10^{-5}). (B) Artificial calculated and imported spectra of enzyme intermediates: (b) E_M form of native GSAT (imported); (c) putative Schiff base of GSA (calculated); (d) central enzyme complex E_L-X (imported from computer simulation of the spectrophotometric reaction of ALA with E_M, data not shown); similar to steady-state spectrum at ~1.5 s, Figure 1C; (e) E_L form of GSAT (calculated); (f) putative ALA ketimine E_M-ALA (imported, similar to curve b). (C) Calculated semi-log time-dependent concentrations of reactant (a) and product (h) and various putative enzyme intermediates as noted in panel B. (Inset) zoom of concentration changes observed during early stages of the global analysis.

spectra provided sufficient constraints to allow successful fitting to original data sets (Figure 1A). Resulting calculated artificial time-dependent spectra are shown in Figure 6A (variance of 4.2×10^{-5}). Spectra of various intermediates and their calculated time-dependent concentration profiles are shown in Figure 6, panels B and C. During initial stages of the reaction, a (GSA) combines quantitatively with b, whose spectrum is that of aminic enzyme, E_M. The resulting binary enzyme intermediate c (E_M-GSA) is similar to that observed in the original data set (Figure 1B). Its artificial spectrum was generated during simulation. This intermediate was gradually converted to d (E_L-X), whose spectrum was imported from ALA computer simulations described previously. The subsequent formation of e (E_L) and its calculated artificial spectrum is similar to that observed in Figure 1C. These enzyme intermediates gradually approached their steady-state concentrations (1−2 s), and only insignificant increases in g and h (ALA) were obtained. This stage is followed by the steady-state conversion of a (GSA) to h (ALA) and subsequent regeneration of b (E_M), not obvious in Figure 6C.

Assignment of observed spectral changes to specific enzyme intermediates (Scheme 3) and comparison with artificial computer simulated graphics is speculative and based largely on circumstantial evidence derived from various types of experiments. Nevertheless, such tentative assignments are particularly instructive in the present context.

Comparison of Transient-State Parameters with k_{cat} and K_M. The minimal mechanism and associated constants were further evaluated by comparison with corresponding steady-state parameters. If one assumes that effects due to the dissociation of DAVA from the central enzyme complex are relatively small, then Scheme 2 becomes a simple four step linear mechanism with k_{cat} and K_M defined by eqs 7 and 8 (*17*).

$$k_{cat} = \frac{k_{+2}k_{+3}k_{+4}}{(k_{+2} + k_{-2})(k_{-3} + k_{+4}) + k_{+2}k_{+3} + k_{+3}k_{+4}} \quad (7)$$

$$K_M = \frac{k_{-1}[k_{-2}(k_{-3} + k_{+4}) + k_{+3}k_{+4}] + k_{+2}k_{+3}k_{+4}}{k_{+1}[(k_{+2} + k_{-2})(k_{-3} + k_{+4}) + k_{+2}k_{+3} + k_{+3}k_{+4}]} \quad (8)$$

Substitution of calculated values for each of the constants (from Scheme 3) into the above equations yields 3 s^{-1} and 1.6×10^{-5} M for k_{cat} and K_M, respectively. These compare with steady-state values of 1 s^{-1} and 1.2×10^{-5} M, respectively (*7*).

DISCUSSION

Solution of an enzyme mechanism must include fitting experimental data of various types to a model, with the expectation that the results will converge to a single solution, without simplifying assumptions. The challenge becomes one of establishing a minimal kinetic scheme. The scheme used in the present kinetic analysis is based on (a) the generally accepted mechanism of amino transfer (*13*, *14*), (b) spectral characteristics of expected intermediates, (c) singular value decomposition factor analysis (SVD), and (d) computer simulation of GSAT catalyzed spectrophotometric reactions with ALA and DAVA.

Spectrophotometric Analyses. In reactions with GSA, DAVA, or ALA, the first spectrum observed after rapid mixing is indistinguishable from that of the initial aminic or aldiminic form of GSAT. On the basis of the results of Briley et al. (*21*) and Sterk and Gehring (*22*) with aspartate aminotransferase, which has served as a kinetic model in many studies with GSAT (*6*, *7*, *16*, *23*), it is not unreasonable to assume that collision complexes of GSAT are not directly observed in experiments described here with natural substrates. This being the case, spectral changes observed after rapid mixing (Figure 1B) are likely associated with Schiff base formation (*20*), although exceptions with substrate analogues have been noted (*22*). Initial spectral changes to shorter wavelengths observed with aspartate aminotransferase have been similarly associated with ketimine or external

aldimine formation (*21*, *22*). In this sense, GSAT is a good model since several intermediates, including minor quinonoid-like forms (*6*), can be transiently observed at room temperature.

The second spectral change observed (Figure 1C) is likely associated with ketimine/aldimine tautomerization. The minimal mechanism includes two such 1,3-prototropic rearrangements, one leading to formation of the external aldimine of DAVA and the other to the formation of the ketimine of ALA (Scheme 2, reactions 2 and 3 and 6 and 7). If proton abstraction (reactions 2 and 6) is rate limiting as previously suggested (*20*), then transient accumulation of the Schiff base of GSA (E_M-GSA) and the external aldimine(s) of DAVA (E_L-DAVA) is expected [along with other enzyme intermediates with which either of these might be in rapid equilibrium, such as cyclic geminal diamines ($E_L=$DAVA]. This is consistent with observed transient absorbance increases at 326 and subsequently 418 nm (Figure 1, panels B and C, respectively).

Minor quinonoid-like intermediates (490−530 nm) have been ignored in the present study. Nevertheless, they are likely intermediates in GSAT-catalyzed tautomerizations. They are transiently dominant in reactions of (a) GSA with aldiminic enzyme, (b) DOVA with aminic enzyme (*6*), and (c) ALA with aldiminic enzyme plus low molecular weight nitrogenous base (data not shown) (Scheme 1, reactions 10, 11, and 15, respectively). It is not likely that the enzymic mechanism is different in these reactions. Rather, it is more reasonable to suppose that increased stability of these quinonoid-like structures is due primarily to extended double bond conjugation, including the C-4 and C-5 carbonyls of ALA and GSA. This results in additional resonance stabilized intermediates (*7*). Minor absorbance increases observed in the 490−530 nm range (Figure 1, panels C and D) certainly indicate quinonoid intermediates. The transient appearance of an isosbestic point (∼468 nm) during final stages of the reaction with GSA (Figure 1D) is consistent with this hypothesis, in which case the C-4 quinonoid of ALA should predominate over its C-5 GSA isomer. The C-5 quinonoid would be more likely under pre-steady-state conditions. Indeed an isosbestic point is also observed during very early stages of the reaction (not apparent in Figure 1B), but not during steady-state, probably because of the heterogeneity of isomeric quinonoids and aldimine-related enzyme intermediates.

Rapid Equilibrium of External Aldimines and Geminal Diamines. In the case of GSAT, establishing a minimal mechanism is complicated by the large number of reactions known to occur with the single substrate GSA (Scheme 1), several of which have near identical spectral properties. Simplifying assumptions, therefore, have been absolutely essential. Little progress was made until it was realized that isomeric external aldimines of DAVA (with either C-4 or C-5 amino group) and corresponding diamines (cyclic imidazolidines) are likely in rapid equilibrium (Figure 5). This being the case, kinetic analyses are greatly simplified because these intermediates can then be grouped into a single enzyme complex (E_L-X) with physical and enzymic characteristics defined by constituent concentration ratios. Steady-state, transient-state, and equilibrium titration experiments with enzyme-free pyridoxal-5′-phosphate and mutant (Lys272Ile) GSAT all appear to vindicate this rapid equilibrium assumption.

In enzyme-free reactions with PLP and saturating concentrations of DAVA, it would appear that this equilibrium favors formation of the cyclic imidazolidine by about 1−2, based on molar extinction coefficients (*7*). In this case, only minimal amounts of internal aldimine (λ_{max} also ∼418 nm) are expected. In the case of the Lys272Ile mutant, the apparent ratio of ∼330:415 nm absorbance is clearly dependent on DAVA concentration (Figure 5). In simulated spectrophotometric reactions with DAVA, 415 nm absorbance predominates (curve c in Figure 4B), while simulations with ALA indicate roughly equal amounts of 330 and 415 nm absorbance in the putative heterologous central enzyme complex (E_L-X) (data not shown). The apparent steady-state spectrum (last spectrum, Figure 1C) is practically superimposable with that obtained in simulations with DAVA (Figure 4B). The ratio of imidazolidine to external aldimines in the synthesis of ALA is difficult to estimate. We have used the spectrum obtained from ALA simulation reactions. The simulation of the minimal mechanism and associated constants suggests significant amounts of internal aldimine (curve e in Figure 6C, inset) during steady-state.

Ketoenamine/enolimine tautomers are purportedly also involved in transamination reactions. Prior to or synchronously with quinonoid formation a proton purportedly shifts from the imine nitrogen (430 nm) to the phenolic oxygen (330 nm) (*24*). The existence of such tautomers might further complicate correct interpretation of the present spectrophotometric data.

Rapid equilibrium of aldimines and geminal diamines (rate constants $\approx 10^5$ s^{-1}) provides a reasonable explanation of the above experimental results and is consistent with the observation that intramolecular transimidation are purportedly 10^7 larger than reactions requiring Schiff base hydrolysis and reformation (*15*). Most importantly, this putative heterologous complex provides the basis for a unifying hypothesis essential to understanding the mechanism of GSAT and perhaps its regulation.

Neglecting Secondary Reactions. Equally important is the assumption that secondary reactions are negligible, i.e., reactions of GSA and ALA with E_L or the internal aldimine of GSAT (Scheme 1, reactions 9 and 16). Since the overall kinetic strategy begins at the three ends of the branched pathway and works toward the middle, this assumption relates to the significance of secondary reactions during the formation of E_L-X in transient- or pre-steady-state reactions with GSA or DAVA or ALA. Time-dependent concentration profiles of putative enzyme intermediates in simulated reactions of GSA (Figure 6C), DAVA (Figure 4C), and ALA (not shown) are consistent with this hypothesis. For example, in the reaction of DAVA with E_L, stoichiometric formation of the putative central enzyme complex E_L-X (curve c in Figure 4C) occurs long before ALA (curve f in Figure 4C) is available for secondary reaction with E_L. Nevertheless, the high concentration of ALA required to drive the reverse reaction, the relatively high affinity of ALA for aldiminic GSAT (E_L) (*6*), and abortive complex formation are matters of concern.

Evaluating the Minimal Reaction Mechanism. We have attempted to vindicate the minimal mechanism and associated kinetic parameters (Scheme 3) by computer simulation, by

their internal consistency, by comparison with steady-state parameters, and by direct equilibrium experiments. For example, computer generated time-dependent spectra (Figure 6A) using the minimal mechanism and associated constants (Scheme 3) is similar (variance $\sim 10^{-5}$) to transformed spectra obtained from the original GSA data-set (Figure 1A). On the basis of maximum amplitudes this represents an average of ~4% error.

The dissociation constant (K_d) for GSA (Scheme 3) which is given by the ratio of the rate constants (k_{-1}/k_{+1}) is $\sim 5 \times 10^{-5}$ M (11.3 s^{-1}/2.36 $\times$ 10^5 s^{-1} M^{-1}). This compares favorably with $\sim 7 \times 10^{-5}$ M, which is obtained from other transition-state relationships (eq 3):

$$K_d \approx K_{d,app}\,(k_{+2} + k_{-2})/k_{-2} = 4.98 \times 10^{-6}\ \mathrm{M}(7.36\ s^{-1} + 2.80\ s^{-1})/7.36\ s^{-1}$$

The apparent dissociation constant ($K_{d,app}$) is defined by a hyperbola, fit to the concentration dependence of the second apparent rate constant (k_{2obs}) (see Experimental Procedures).

Further credibility of the minimal reaction mechanism was obtained by comparison of k_{cat} and K_M, calculated from transition-state (3 s^{-1}, 1.6×10^{-5} M, respectively; eqs 7 and 8, respectively) and steady-state data (1 s^{-1} and 1.2×10^{-5} M, respectively) (*7*). The larger value for k_{cat}, calculated from transient-state kinetic data, is likely a consequence of the assumption that dissociation of the central enzyme complex (E_L−X), and resulting formation of free aldiminic enzyme E_L and DAVA, is negligible. Computer simulations indicate a significant fraction of E_L during steady state (curve e in Figure 6C, inset) and that the rate of ALA formation is very sensitive and inversely proportional to the corresponding apparent dissociation constant (see Scheme 3, 16.3 s^{-1}/(135 s^{-1} $\times$ 3.64 $\times$ 10^{-3} μM^{-1}).

The equilibrium constant calculated from pre-steady-state data (Scheme 3) is ~1200. It is crucial to corroborate this value directly with equilibrium experiments. To date, this has not been possible, due primarily to the instability of GSA to reaction conditions (*7*, *25*). The difficulty of separating GSA from its isomeric product (ALA) with sufficient resolution to determine concentration ratios in the range of ~1:1200 is also problematic. Equilibration experiments of the reverse reaction of GSAT with [^{14}C]ALA have been similarly unsuccessful. Nevertheless, reasonably consistent values have been obtained in equilibrations of DAVA and ALA (data not shown). On the basis of transient-state experiments, K_{eq} for this half-reaction is ~660 (Scheme 3; $[ALA][E_M]/[DAVA][E_L] = k_{-5}k_{+6}k_{+7}k_{+8}k_{+9}/k_{+5}k_{-6}k_{-7}k_{-8}k_9$). A value of ~200 was obtained in preliminary equilibrium titration experiments (data not shown).

This consistency among various experimental techniques indicates that the minimal mechanism (Scheme 3) provides a reasonable description of GSAT catalysis. Observed differences are understandable when one considers the complexity of the reactions (Scheme 1) and various experimental limitations. For example, the instability of GSA under reaction conditions, particularly at higher concentrations, raises serious questions about effective versus actual substrate concentrations. In addition, DAVA reacts nearly quantitatively with E_L (*16*) and therefore pseudo-first-order extrapolations ($[E_L] \ll [DAVA]$) to zero substrate concentration are inherently problematic (Figure 3B). In addition, effects of the *R* enantiomer in racemic solutions of DAVA have not been considered, etc.

Regulation of GSAT. This brings us directly to another idiosyncracy of GSAT, i.e., very gradual re-equilibration of enzyme intermediates during final stages of the reaction with GSA (Figure 1, >20 s). The absorbance at ~338 nm (aminic-like enzyme) once again decreases ($k_{app} \approx 0.012\ s^{-1}$) with concomitant increases at ~418 nm (aldiminic-like GSAT). The apparent rate constant for this equilibration (data not shown) is a linear function of the initial GSA concentration. This represents an unexpected confirmation of a branched minimal mechanism (Scheme 2, reactions 4 or 5), suggesting thermodynamically driven dissociation of the central enzyme complex (E_L−X). As mentioned previously, computer simulations indicate that this dissociation is a very sensitive indicator (inversely proportional) of the rate of ALA synthesis. This is in agreement with steady-state experiments which show that DAVA and higher GSAT concentrations increase k_{cat} (*7*, *12*). Given the relatively high affinity of ALA for aldiminic enzyme (E_L) (*6*) and the steady-state accumulation of this reaction product, gradual absorbance increases at ~418 nm as the reaction approaches equilibrium might indicate formation of the external aldimine of ALA (E_L−ALA), previously referred to as a secondary reaction (reaction 16 of Scheme 1). This external aldimine is a dead-end binary, covalent enzyme intermediate. Unlike GSA, ALA does not give characteristic tautomeric spectral changes with E_L. Nevertheless, ALA is known to inhibit the reaction of gabaculine with this enzyme form (*23*). This may have important implications in terms of biological regulation of GSAT.

Uptake of ALA by plants leads to accumulation of photosensitive tetrapyrrole precursors. Elevated synthesis or an external supply of ALA reduces steady-state levels of GSAT-specific RNA by a feedback regulatory mechanism (*26*). It is reasonable to assume that ALA accumulation might also be post-translationally regulated.

Finally, in spite of obvious limitations, transient-state kinetic analysis provides an important confirmation of the minimal reaction mechanism of GSAT. This mechanistic model is relatively simple, reflects the generally accepted mechanism of amino transferases, is consistent with steady-state and equilibrium experiments, and it provides an innovative mechanism for the potential biological regulation of this important enzyme.

ACKNOWLEDGMENT

The assistance of my wife Grace Marie in proofreading this and *all* other manuscripts over the years of my (M.A.S.) career in biochemistry is gratefully acknowledged!

REFERENCES

1. Beale, S. I., and Weinstein, J. D. (1990) in *Biosynthesis of Heme and Chlorophyll* (Dailey, H. A., Ed.) pp 287−391, McGraw-Hill, New York.
2. Kannanagara, C. G., Andersen, R. V., Pontoppidan, B., Willows, R., and von Wettstein, D. (1994) in *The Biosynthesis of the Tetrapyrrole Pigments* (Chadwick, D. J., and Ackrill, K., Eds.) pp 21−39, Wiley, Chichester.
3. Smith, A. G., and Griffiths, W. T. (1993) in *Methods in Plant Biochemistry* (Dey, P. M., and Harborne, J. B., Eds.) Vol. 9, pp 299−344, Academic Press, London.

4. Grimm, B. (1990) *Proc. Natl. Acad. Sci. U.S.A. 87*, 4169−4173.
5. Elliot, T., Avissar, Y. J., Rhie, G.-E., and Beale, S. I. (1990) *J. Bacteriol. 172*, 7071−7084.
6. Smith, M. A., Grimm, B., Kannangara, C. G., and von Wettstein, D. (1991) *Proc. Natl. Acad. Sci. U.S.A. 88*, 9775−9779.
7. Smith, M. A., Kannangara, C. G., Grimm, B., and von Wettstein, D. (1991) *Eur. J. Biochem. 202*, 749−757.
8. Gehring, H., Christen, P., Eichele, G., Glor, M., Janonius, J. N., Reimer, A. S., Smit, J. D. G., and Thaller, C. (1977) *J. Mol. Biol. 115*, 97−101.
9. Grimm, B., Smith, M. A., and von Wettstein, D. (1992) *Eur. J. Biochem. 206*, 579−585.
10. Gough, S. P., Kannangara, C. G., and Bock, K. (1989) *Carlsberg Res. Commun. 54*, 99−108.
11. Grimm, B., Smith, A. J., Kannangara, C. G., and Smith, M. A. (1991) *J. Biol. Chem. 266*, 2494−12501.
12. Tyacke, R. T., Harwood, J. L., and John, R. (1993) *Biochem. J. 293*, 697−701.
13. Fasella, P., and Turano, C. (1970) *Vitamin Hormones*, Vol. 28, pp 157−194, New York.
14. Arnone, A., Christen, P., Jansonius, J. N., and Metzler, D. E. (1985) in *Transaminases* (Christen, P., and Metzler, D. E., Eds.) pp 326−357, Wiley, New York.
15. Tobias, P. S., and Kallen, R. G. (1975) *J. Am. Chem. Soc. 97*, 6530−6539.
16. Smith, M. A., Kannangara, C. G., and Grimm, B. (1992) *Biochemistry 31*, 11249−11254.
17. Johnson, K. A. (1992) in *The Enzymes* (Sigman, D. S., Ed.) Vol. XX, pp 1−61, Academic Press, Inc., New York.
18. Benson, S. W, (1960) *The Foundations of Chemical Kinetics*, McGraw-Hill, New York.
19. Tybus, K. M., and Taylor, E. W. (1982) *Biochemistry 21*, 1284−1994.
20. Kirsch, J. F., Eichele, G., Ford, G. C., Vincent, M. G., Jansonius, J. N., Gehring, H., and Christen, P. (1984) *J. Mol. Biol. 174*, 497−525.
21. Briley, P., Eisenthal, R., Harrison, R., and Smith, G. D. (1977) *Biochem. J. 161*, 383−387.
22. Sterk, M., and Gehring, H. (1991) *Eur. J. Biochem. 201*, 703−707.
23. Smith, M. A., and Grimm, B. (1992) *Biochemistry 31*, 4122−4127.
24. Chen, V. J., Metzler, D. E., and Jenkins, W. T. (1987) *J. Biol. Chem. 262*, 14422−14427.
25. Pugh, C. E., Harwood, J. L., and John, R. (1992) *J. Biol. Chem. 267*, 1584−1588.
26. Zargorodnyaya, A., Papenbrock, J., and Grimm, B. (1997) *Plant J.* (in press).

BI9717587